Extended Abstracts of the 18th (1986 International) Conference on Solid State Devices and Materials, Tokyo, 1986, pp. 415-418

Investigation on Microarea Stress in Silicon by Microprobe Raman Spectroscopy

S.Kambayashi, T.Hamasaki, T.Nakakubo*, M.Watanabe, and H.Tango

Toshiba Corp. VLSI Research Center, Total Information System Div.*
1 Komukai-Toshiba-cho, Saiwai-ku, Kawasaki 210, JAPAN

Stress in 1 μm diameter spot area of a silicon wafer with a silicon V-groove structure covered with silicon dioxide was analyzed by using the Raman microprobe technique. The stress in the space between two grooves was measured to be $8x10^8$ dyn/cm^2, whereas no stress was observed in a non-grooved area.

Simulation, using the finite element method, was carried out to obtain thermal stress distribution around the groove structure. The simulated results agreed qualitatively with the microarea stress measurements.

These techniques enable investigating local stresses which will induce crystal defects in the device fabrication process.

1. Introduction

Semiconductor device geometries have shrunk in accordance with the reduced scaling law for the high packing density VLSIs. In non-planar geometry, such as a trench capacitor or LOCOS isolation, defects in silicon will be induced due to local stress concentrated in a small silicon wafer area during device processing. It will become a serious problem for sub-micron VLSIs.

On the other hand, Raman spectroscopy has been used for investigation of stress in single crystal silicon. A Raman spectrum for silicon (TO, transverse optical band) has been used to analyze stress in silicon-on-sapphire[1,2]. Recently, the Raman microprobe technique has been proved to be applicable for the characterization of recrystallization and crystal orientation of silicon with a high spatial resolution[3,4]. This is considered to be useful in directly measuring local stress in silicon.

Stress is induced within a microarea in a silicon wafer during the device fabrication process, because of the difference in thermal expansion coefficients between silicon and silicon dioxide. The stress varies strongly, depending on the geometrical structure for non-planer devices. This paper reports on the local stress distribution in microfabricated silicon wafers, measured by using the Raman microprobe technique, and discusses the stress variation, combined with thermal stress simulation using the finite element method.

2. Experiments

Raman spectra were measured at room temperature using a triple monochromator(JEOL TRS-400T) with a microscope attachment. The 4880Å line for an argon-ion laser was used for sample excitation. The excitation laser beam was focused into a one-micron diameter spot with the microscope. Back-scattered light was detected by a photon counting system, combined with a personal computer. It was possible to observe the excitation area position in a sample under 1000 times magnification and select the area for spectrometric measurements. The observed Raman frequency shift was calibrated by the neon line, as shown in Fig. 1. The Raman spectra were scanned from low to high frequencies. Both the Raman spectra for silicon and neon line (19979.4 cm^{-1}) were obtained within one scanning. The Raman shift was measured with reproducible accuracy better than 0.1 cm^{-1}.

The sample excitation area was heated by the irradiation of high energy density laser beam focused into a very small area. The Raman frequency change in single crystal silicon with temperature has been reported by Hart et al[5]. In order to avoid this temperature effect, in this study, the excitation laser power used was

3mW.

Samples were prepared in the following way. Grooves on the (100) silicon wafer surface were made by KOH chemical etching, using a silicon dioxide mask. Silicon dioxide films 0.9 um thick were deposited by the low pressure chemical vapor deposition technique(LPCVD) at 430°C onto the silicon wafer after the silicon dioxide mask removal. The LPCVD silicon dioxide films on the back of the silicon wafer were removed by chemical etching. These samples had very little damage, due to making grooves by chemical etching. Raman spectra for silicon were measured on the (110) plane carefully cleaved, so as not to induce additional stress, as shown in Fig. 2.

It has been known that, in the presence of uniaxial stress the Raman peak for silicon (around 520 cm^{-1}) splits and shifts linearly with stress[6]. In this study, back-scattering geometry was used for Raman spectra measurement on the (110) surface of silicon. Incident and scattered lights propagated along the [110] direction of the silicon crystal. The incident light was polarized along the [110] axis of the silicon crystal. The back-scattered radiation, almost polarized along the [110] axis, was entered into the spectrometer since the half-mirror has a polarizer property. When the

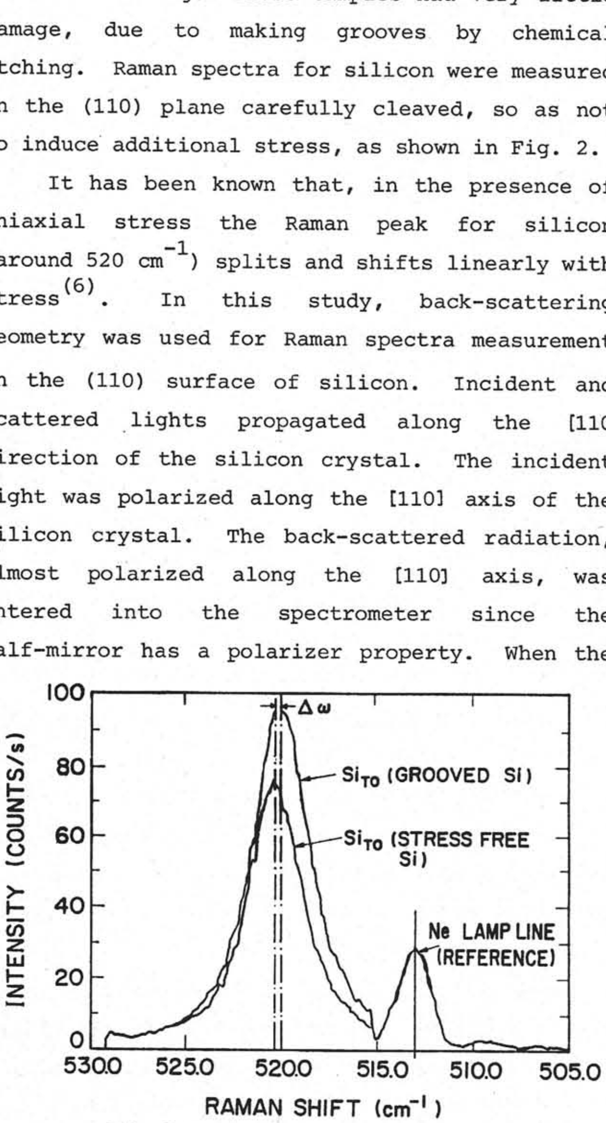

Fig.1 Typical Raman spectra.

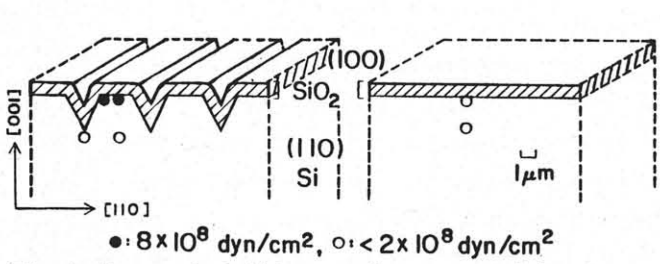

Fig.2 Stress in silicon wafer measured by Raman microprobe technique.

measurements were performed in this Raman back-scattering configuration for [110] stress, the stresses were determined from the observed frequency shift using the following equation derived by Englert et al[1].

$$\sigma = 2.49 \times 10^9 \times \Delta\omega \ (dyn/cm^2) \qquad (1)$$

where σ is the stress in the excitation area and $\Delta\omega(cm^{-1})$ is the change in the observed Raman frequency shift, as shown in Fig. 1.

3. Results and discussion

3.1 Raman microprobe analysis

The measurement point positions in the sample are indicated in Fig. 2. At the points in which Raman frequency change were observed, stresses component seemed to be parallel to the sample surface. Therefore, the stress could be calculated from the observed frequency change, using Eq.(1). The obtained local stress values are shown in Fig. 2. The $(8\pm2)\times10^8$ dyn/cm² tensile stress was observed at the center between two grooves at the surface of the silicon wafer, but stress was not detected at any surface area without a groove structure.

Stress at points without grooves in a silicon wafer is calculated from the silicon wafer radius of curvature[7], since the LPCVD silicon dioxide films exist only on one side of the wafer surface. The radius of curvature for samples was 6×10^3 cm, this radius of curvature was same to that of samples without grooves. The stress values, calculated from the radius of

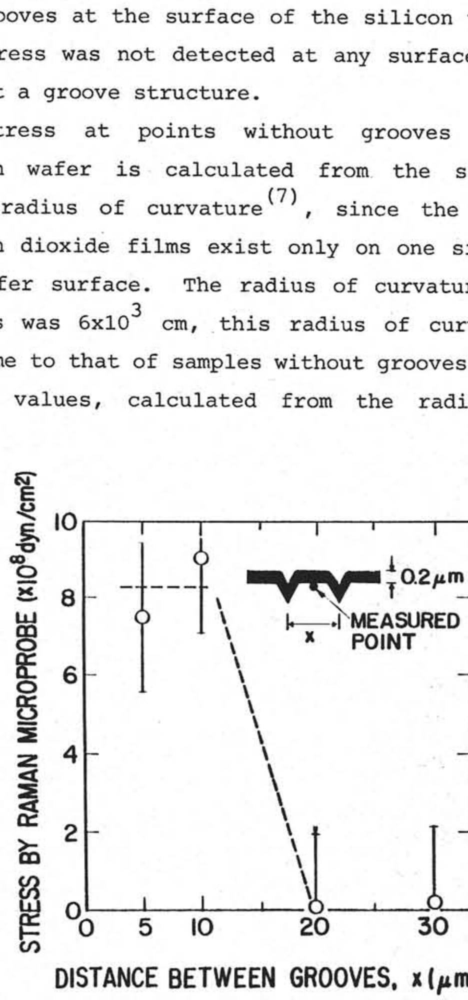

Fig.3 Stress at the center between V-grooves measured by Raman microprobe technique.

curvature at the surface of the silicon wafer with a 0.9 μm thick silicon dioxide film, was 1.2 x 10^7 dyn/cm^2. For the sample without grooves, this stress values was small enough not to be ditected by the Raman microprobe technique as shown in Fig. 2.

Figure. 3 shows the variation in the stress at the surface of the silicon wafer at the center between the V-grooves as a function of distance between the two grooves. It is clearly shown that the stresses between the two grooves decreased rapidly with the increase in distance between the two grooves.

3.2 Thermal stress simulatin

The local stress in a silicon crystal with a micro structure can not be calculated from the radius of curvature for a silicon wafer. Therefore, it is necessary to compute local stresses by the finite element method. Stresses measured by the use of the Raman microprobe technique were compared to this computer simulation.

The finite element method is a discretization method. According to the finite element method, the whole area to be analyzed is divided into a finite number of small areas, that are called "elements", and displacement field in each element is approximated by a shape function which is expressed by the displacement of nodes on this element. The detailed procedure is as follows;

(1) Genelate individual subdivided element matrices by using the variational method.

(2) Calculate nodal displacement by solving linear algebraic equations, which are created by assembling individual element matrices.

(3) Compute individual element displacement fields by using the obtained nodal displacement and calculate stress and strain field.

Recently, the finite element method has become the most frequently used discretization method in structural analysis.

The thermal stress field, caused by differences in thermal expansion coefficients between silicon and silicon dioxide, were computed. A general purpose finite element program MARC(Nippon-MARC Co.) was used.

Generally speaking, the solution accuracy obtained by using the finite element method is limited by the element size and also by inaccuracies in the shape function for each element. To improve accuracy, the area was divided, where expected stress variation was large(i,e, neighborhood of contact surface between silicon and silicon dioxide), into smaller elements than other areas and an element type was adopted whose shape function could represent the second order displacement field (i.e. 8 node element). The stress field was assumed to be under a generalized plane strain state. The configurlation analyzed is shown in Fig. 4. Because this configurlation was assumed to be repeated infinitely within the measurement plane, periodic boundary conditions were imposed at the left and right side edges.

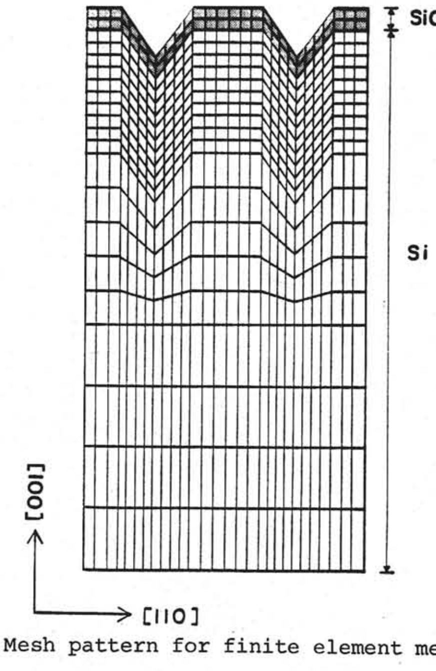

Fig.4 Mesh pattern for finite element method.

The parameters in this computer simulation were as follows. The linear thermal expansion coefficient and Young's modulus for the silicon dioxide film used values for thermally oxidized silicon, which were 5.5×10^{-7} and 7.0×10^{11} dyn/cm^2, respectively[8]. Poisson's ratio for the silicon dioxide film used was 0.45. Young's moduli (E) for silicon were $E_1 = 1.7 \times 10^{12}$ dyn/cm^2, $E_2 = 1.3 \times 10^{12}$ dyn/cm^2. Poisson's ratios (ν) for silicon were $\nu_1 = 0.36$ and $\nu_2 = 0.28$[9]. Subscripts 1 and 2 indicate the directions along the <110> and <100> , respectively. The linear thermal expansion coefficient was 3.0×10^{-6} [10].

Only thermal stresses in the samples could be simulated, for the case when the temperature dropped from 430°C, at which silicon dioxide films were deposited, down to 25°C.

For a non-grooved sample, computed stresses, σ_1 in a 0.9 µm thick silicon dioxide film and near the surface of silicon, were 1.2×10^9 dyn/cm^2 and 5.8×10^7 dyn/cm^2, respectively. On the other hand, computed stress σ_1 in silicon at the central point between two grooves, which were separated by 6 µm distance, was 3.4×10^8 dyn/cm^2, that is, σ_1 became 6 times larger than that for the sample without grooves.

These simulation results were in qualitative agreement with stresses distribution obtained by the Raman microprobe technique. The difference between measurement and simulation due to inaccuracy in the physical parameters of the silicon dioxide film and stresses other than thermal one.

The defect density of the silicon crystal seemed to be proportional to the octahedral shearing stress. The octahedral shearing stress distribution was calculated from the computed thermal stresses, as shown in Fig. 5. Defects will exist in the bottom of the V-groove and near the flat surface of the groove space, when thermal stresses are large.

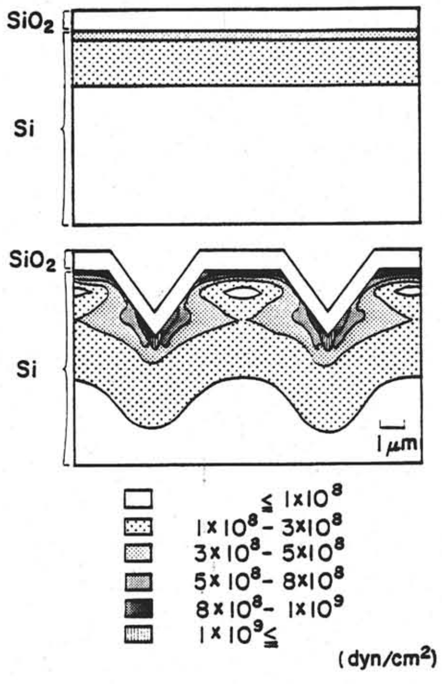

Fig.5 Octahedral shearing stress in a silicon wafer, analyzed by computer simulation, using the finite element method.

4. Conclusion

Local stress in 1um diameter area in a silicon wafer was analyzed by using the Raman microprobe technique.

Stresses were detected around the V-grooved structure wafer covered with silicon dioxide film 0.9 µm thick. The measured stress values at the central point between the V-grooves, 3 µm in depth and 5 and 10 µm groove separations, were $(8 \pm 2) \times 10^8$ dyn/cm^2.

The Raman microprobe tequnique does not have spacial resolution better than 1 µm, while simulation of stresses have uncertainty due to physical parameters. It is well demonstrated combination of these techniques supplement each other and make it possible to investigate stress distribution in sub-micron geometry. This will be useful for reduction of process-induced crystal defects.

References

1)Th.Englert, G.Abstreiter and J.Pontcharra, Solid-State Elec. 23 (1980) 31.

2)Y.Ohmura, T.Inoue and T.Yoshii, Solid State Commun. 37 (1981) 583.

3)S.Nakashima, Y.Inoue, M.Miyauchi and A.Mitsuishi, J. Appl. Phys. 54 (1983) 2611.

4)S.Nakashima, Y.Inoue and A.Mitsuishi, J.Appl. Phys. 56 (1984) 2989.

5)T.R.Hart, R.L.Aggarwal and Benjamin Lax, Phys. Rev.B 1 (1970) 638.

6)E.Anastassakis, A.Pinczuk, E.Bernstein, F.H.Pollak and M.Cardona, Solid State Commu. 8 (1970) 133.

7)R.J.Jaccodine and W.A.Schlegel, J. Appl. Phys. 37 (1966) 2429.

8)T.Tokuyama, Y.Fujii, Y.Sugita and S.Kishino, Jpn. J. Appl. Phys. 6 (1967) 1252.

9)W.A.Brantley. J. Appl. Phys. 44 (1973) 534.

10)"Thermophysical Properties of Matter, Vol.13, 154 (IFI/PLENUM, New-York).